Supporting Information

Title: Molecular basis for the maintenance of lipid asymmetry in the outer membrane of *Escherichia coli*

Authors: Jiang Yeow[a,b,1], Kang Wei Tan[a,1], Daniel A. Holdbrook[c,1], Zhi-Soon Chong[a], Jan K. Marzinek[c,d], Peter J. Bond[c,d,*], Shu-Sin Chng[a,e,*]

Affiliations:

[a]Department of Chemistry, National University of Singapore, Singapore 117543.

[b]National University of Singapore Graduate School for Integrative Sciences and Engineering (NGS), Singapore 117456.

[c]Bioinformatics Institute, Agency for Science, Technology, and Research (A*STAR), Singapore 138671.

[d]Department of Biological Sciences, National University of Singapore, Singapore 117543.

[e]Singapore Center for Environmental Life Sciences Engineering, National University of Singapore (SCELSE-NUS), Singapore 117456.

[1]These authors contributed equally to this work.

*To whom correspondence should be addressed. E-mail: chmchngs@nus.edu.sg, peterjb@bii.a-star.edu.sg

Supplementary Materials and Methods

Bacterial strains and plasmids. All strains and plasmids used are listed in Table S1 and S2, respectively.

Growth conditions. Luria Bertani (LB) broth and agar were prepared as described previously (1). Unless otherwise noted, ampicillin (Amp) (Sigma-Aldrich, MO, USA) was used at a concentration of 200 μg/mL, chloramphenicol (Cam) (Alfa Aesar, Heysham, UK) at 15 μg/mL, kanamycin (Kan) (Sigma-Aldrich) at 25 μg/mL, and spectinomycin (Spec) (Sigma-Aldrich) at 50 μg/mL. For crosslinking experiments, *para*-Benzoyl-L-phenylalanine (*p*Bpa; Alfa Aesar) was dissolved in 1 M NaOH at 0.25 M, and used at 0.25 mM unless otherwise mentioned.

Plasmid construction. To construct most plasmids, the desired gene or DNA fragments were amplified by PCR from the DNA template using primers listed in Table S3. Amplified fragments were digested with relevant restriction enzymes (New England Biolabs) and ligated into the same sites of an appropriate plasmids using T4 DNA ligase (New England Biolabs). NovaBlue competent cells were transformed with the ligation products and selected on LB plates containing appropriate antibiotics. All constructs were verified by DNA sequencing (Axil Scientific, Singapore).

Construction of chromosomal *ompC* mutants using negative selection. All chromosomal *ompC* mutations were introduced via a positive-negative selection method described previously (2). To prepare electro-competent cells, strain MC4100 harbouring pKM208 (3) grown overnight at 30 °C was inoculated into 15 mL SOB broth with 1:100 dilution. Cells were grown at the same temperature until OD_{600} reached ~0.3-0.4. 1 mM of IPTG was added and the culture was grown for another 60 min at 30 °C. Cells were then subjected to heat

shock at 42 °C for 15 min, followed by incubation for 15 min on ice, with intermittent agitation. Subsequently, cells were centrifuged at 5000 x *g* for 10 min and made competent by washing twice with prechilled sterile water followed by cold 10 % glycerol. Competent cells were pelleted and resuspended in cold 10 % glycerol. For positive selection, 1 µg *kan-PrhaB-tse2* cassette amplified from pSLC-246 (2) using ompC_NS_N5 and ompC_NS_C3 primer pairs was transformed into the competent cells using 1-mm electroporation cuvettes (Biorad) in Eppendorf Eporator® (Eppendorf) with an output voltage of 1800 V. Cells were recovered in LB with 2 % glucose at 37 °C for at least 4 h, plated onto LB plates supplemented with Kan and 2 % glucose, and incubated at 37 °C for 24 h. For negative selection, 1 µg PCR product of *ompC* wild-type or mutant constructs amplified using ompC_NS_N5_C and ompC_NS_C3_C primer pairs were transformed into competent cells made from positive selection using similar procedures. After transformation, cells were plated onto minimal (M9) plates supplemented with 0.2 % rhamnose, and incubated for 48 h at 37 °C. Surviving colonies were PCR screened and verified by DNA sequencing (Axil Scientific, Singapore).

In vivo photoactivable crosslinking. We adopted previously described protocol (4) for all in vivo photoactivable crosslinking experiments. Briefly, amber stop codon (TAG) was introduced at selected positions in either pDSW206*ompC* or pCDF*mlaA-His* plasmids via site directed mutagenesis using primers listed in Table S3. For OmpC crosslinking, MC4100 with Δ*ompC*::*kan* background harbouring p*Sup-BpaRS-6TRN* (5) and pDSW206*ompC* were used. For MlaA crosslinking, MC4100 with Δ*mlaA*::*kan* background harbouring p*Sup-BpaRS-6TRN* (5) and pCDF*mlaA-His* were used. An overnight 5 mL culture was grown from a single colony in LB broth supplemented with appropriate antibiotics at 37 °C. Overnight cultures were diluted 1:100 into 10 mL of the same media containing 0.25 mM *p*Bpa and grown until OD_{600} reached ~1.0. Cells were normalized by optical density before pelleting and resuspended in 1 mL ice cold TBS (20 mM Tris pH 8.0, 150 mM NaCl). Samples were either used directly or irradiated with UV light at 365 nm for 20 min at 4 °C or room temperature. All samples were pelleted again and finally resuspended in 200 µL of 2 X Laemmli buffer, boiled

for 10 min, and centrifuged at 21,000 x *g* in a microcentrifuge for one min at room temperature; 15 μL of each sample subjected to SDS-PAGE and immunoblot analyses.

Over-expression and purification of OmpC-MlaA-His complexes. All proteins were overexpressed in and purified from BL21(λDE3) derivatives. We found that BL21(λDE3) strains from multiple labs do not actually produce OmpC; therefore, to obtain OmpC-MlaA complexes, we deleted *ompF* from the chromosome and introduced *ompC* on a plasmid. OmpC-MlaA-His protein complexes were over-expressed and purified from BL21(λDE3) cells with chromosomal Δ*ompF*::*kan* background co-transformed with either pDSW206*ompC*$_{p\text{Bpa}}$, p*Sup-BpaRS-6TRN* and pCDF*dmlaA-His* (for in vitro crosslinking experiments), or pACYC184*ompC* and pET22b(+)*dmlaA-His* (for characterization of the wildtype complex). An overnight 10 mL culture was grown from a single colony in LB broth supplemented with appropriate antibiotics at 37 °C. The cell culture was then used to inoculate a 1-L culture and grown at the same temperature until OD_{600} reached ~ 0.6. For induction, 0.5 mM IPTG (Axil Scientific, Singapore) was added and the culture was grown for another 3 h at 37 °C. Cells were pelleted by centrifugation at 4,700 x *g* for 20 min and then resuspended in 10-mL TBS containing 1 mM PMSF (Calbiochem) and 30 mM imidazole (Sigma-Aldrich). Cells were lysed with three rounds of sonication on ice (38 % power, 1 second pulse on, 1 second pulse off for 3 min). Cell lysates were incubated overnight with 1 % n-dodecyl β-D-maltoside (DDM, Calbiochem) at 4 °C. Cell debris was removed by centrifugation at 24,000 x *g* for 30 min at 4 °C. Subsequently, supernatant was incubated with 1 mL Ni-NTA nickel resin (QIAGEN), pre-equilibrated with 20 mL of wash buffer (TBS containing 0.025 % DDM and 80 mM imidazole) in a column for 1 h at 4 °C with rocking. The mixture was allowed to drain by gravity before washing vigorously with 10 x 10 mL of wash buffer and eluted with 10 mL of elution buffer (TBS containing 0.025% DDM and 500 mM imidazole). The eluate was concentrated in an Amicon Ultra 100 kDa cut-off ultra-filtration device (Merck Millipore) by centrifugation at 4,000 x *g* to ~500 μL. Proteins were further purified by SEC system (AKTA Pure, GE Healthcare, UK) at 4 °C on a prepacked Superdex 200 increase 10/300 GL column,

using TBS containing 0.025% DDM as the eluent. Protein samples were used either directly or irradiated with UV at 365 nm for in vivo photoactivable crosslinking experiments.

SEC-MALS analysis to determine absolute molar masses of OmpC-MlaA-His complex. Prior to each SEC-MALS analysis, a preparative SEC was performed for BSA (Sigma-Aldrich) to separate monodisperse monomeric peak and to use as a quality control for the MALS detectors. In each experiment, monomeric BSA was injected before the protein of interest and the settings (calibration constant for TREOS detector, Wyatt Technology) that gave the well-characterized molar mass of BSA (66.4 kDa) were used for the molar mass calculation of the protein of interest. SEC purified OmpC-MlaA-His was concentrated to 5 mg/mL and injected into Superdex 200 Increase 10/300 GL column pre-equilibrated with TBS and 0.025 % DDM. Light scattering (LS) and refractive index (*n*) data were collected online using miniDAWN TREOS (Wyatt Technology, CA, USA) and Optilab T-rEX (Wyatt Technology, CA, USA), respectively, and analyzed by ASTRA 6.1.5.22 software (Wyatt Technology). Protein-conjugate analysis available in ASTRA software was applied to calculate non-proteinaceous part of the complex. In this analysis, the refractive index increment *dn/dc* values (where *c* is sample concentration) of 0.143 mL/*g* and 0.185 mL/*g* were used for DDM and protein complex, respectively (6). For BSA, UV extinction coefficient of 0.66 mL/(mg.cm) was used. For the OmpC-MlaA-His complex, that was calculated to be 1.66 mL/(mg.cm), based on its predicted stoichiometric ratio $OmpC_3MlaA$.

Affinity purification experiments. Affinity purification experiments were conducted using Δ*mlaA* strains expressing MlaA-His at low levels from the pET23/42 vector. For each strain, a 1.5-L culture (inoculated from an overnight culture at 1:100 dilution) was grown in LB broth at 37 °C until OD_{600} of ~0.6. Cells were pelleted by centrifugation at 4700 x *g* for 20 min and then resuspended in 10-mL TBS containing 1 mM PMSF (Calbiochem) and 50 mM imidazole (Sigma-Aldrich). Cells were lysed with three rounds of sonication on ice (38 % power, 1 second pulse on, 1 second pulse off for 3 min). Cell lysates were incubated overnight with 1 %

n-dodecyl β-D-maltoside (DDM, Calbiochem) at 4 °C. Cell debris was removed by centrifugation at 24,000 x *g* for 30 min at 4 °C. Subsequently, supernatant was incubated with 1 mL Ni-NTA nickel resin (QIAGEN), pre-equilibrated with 20 mL of wash buffer (TBS containing 0.025% DDM and 80 mM imidazole) in a column for 1 h at 4 °C with rocking. The mixture was allowed to drain by gravity before washing vigorously with 10 x 10 mL of wash buffer and eluted with 5 mL of elution buffer (TBS containing 0.025% DDM and 500 mM imidazole). The eluate was concentrated in an Amicon Ultra 100 kDa cut-off ultra-filtration device (Merck Millipore) by centrifugation at 4,000 x *g* to ~100 μL. The concentrated sample was mixed with equal amounts of 2X Laemmli buffer, boiled at 100 °C for 10 min, and subjected to SDS-PAGE and immunoblot analyses.

Trypsin digestion for protein N-terminal sequencing and mass spectrometry analyses. A 1 mg⁄mL solution of purified OmpC-MlaA-His (OmpC was either wild-type or substituted with *p*Bpa at selected positions) complex was incubated with or without 50 μg⁄mL trypsin (Sigma-Aldrich) for 1 h at room temperature. *p*Bpa substituted samples were irradiated with UV at 365 nm before trypsin digestion. Samples were then analyzed by SDS-PAGE, followed by SEC. Peak fractions from SEC for each sample were pooled, concentrated using an Amicon Ultra 100 kDa cut-off ultra-filtration device (Merck Millipore), and resuspended in 2 X Laemmli sample buffer before analyses by SDS-PAGE and immunoblot using α-MlaA antibody. For N-terminal sequencing, samples were transferred onto PVDF membrane, followed by Coomassie Blue staining (1–2 s). The desired protein bands were carefully excised with a surgical scalpel. For tandem MS, protein bands were excised from a Coomassie Blue stained Tricine gel. Samples prepared for N-terminal sequencing and tandem MS were kept in sterile 1.5 mL centrifuge tubes before submission for analyses at Tufts University Core Facility, Boston, USA, and Taplin Biological Mass Spectrometry Facility, Harvard Medical School, Boston, USA, respectively.

In vivo disulfide bond analysis. Strain NR1216 (Δ*dsbA*) harbouring pET23/42*mlaA-His* expressing MlaA-His with site specific cysteine substitutions was grown overnight in LB broth at 37 °C. A 0.5 mL of overnight culture was normalized by optical density, added with trichloroacetic acid (TCA) at final concentration of ~14 % and mixed thoroughly at 4 °C. This step was performed to prevent scrambling of disulfide bond formed in the cysteines substituted MlaA-His. Proteins precipitated for at least 30 min on ice were centrifuged at 16,000 × *g* for 10 min at 4 °C. The pellet was washed with 1 mL of ice-cold acetone and centrifuged again at 16,000 × *g* for 10 min at 4 °C. Supernatants were then aspirated and the pellet was air dried at room temperature for at least 20 min. Samples were resuspended thoroughly with 100 µL of either 100 mM Tris.HCl pH 8.0, 1% SDS (for non-reduced samples), or the same buffer supplemented with 100 mM of dithiothreitol (DTT) (for reduced samples), incubated for 20 min at room temperature. The samples were finally mixed with 4 X Laemmlli buffer, boiled for 10 min and subjected to SDS-PAGE and immunoblotting analyses using α-His antibody.

Docking of MlaA to OmpC

The ClusPro server (7) was used to dock MlaA (ligand, uniprot ID: P76506, https://gremlin2.bakerlab.org/meta_struct.php?page=p76506) (8) to OmpC (receptor, PDB ID: 2J1N) (9). The default server settings were used in the docking procedure. The minimum distance between 6 residues on OmpC and the corresponding cross-linked peptide regions of MlaA was calculated for all the predicted structures obtained from the server. The OmpC-MlaA model with the smallest average minimum distance of all residue and peptide pairs was selected as the initial structure for use in the all-atom simulations.

Simulation procedures and setup

All simulations were performed using version 5.1.4 of the GROMACS simulation package (10, 11).

All-atom simulations. In total, 6 all-atom simulations were performed (Table A). The simulations were performed using the CHARMM36 force filed parameter set (12). The equations of motion were integrated using the Verlet leapfrog algorithm with a step size of 2 fs. Lengths of hydrogen bonds were constrained with the LINCS algorithm (13). Electrostatic interactions were treated using the smooth Particle Mesh Ewald (PME) method (14), with cutoff for short-range interactions of 1.2 nm. The van der Waals interactions were switched smoothly to zero between 1.0 and 1.2 nm. The neighbor list was updated every 20 steps. The Nose-Hoover thermostat (15, 16) with a coupling constant of 1.0 ps was used to maintain a constant system temperature of 313 K. The protein, membrane and solvent (water and ions) were coupled to separate thermostats. The Parrinello-Rahman barostat (17) with a coupling constant of 5.0 ps was used to maintain a pressure of 1 bar. Semi-isotropic pressure coupling was used for all the membrane systems, while isotropic coupling was used for the solvent-only system. Initial velocities were set according to the Maxwell distribution.

Proteins were inserted into a pre-equilibrated, symmetrical 1,2-dimyristoyl-phosphatidylethanolamine (DMPE) membrane over 5 ns using the membed tool (18) in the GROMACS simulation package. Subsequent equilibration, with position restraints of 1000 kJ mol^{-1} placed on all non-hydrogen protein atoms, was performed for 20 ns to allow the solvent and lipids to equilibrate around the proteins. The position restraints were removed before performing the production runs.

Table A. Summary of all-atom molecular simulations: system compositions and simulation times

Protein Configuration	Lipids	Water and Ions	Simulation time (# of simulations x ns)
MlaA	N/A	9439 H_2O 29 K^+ 19 Cl^-	1 x 500
MlaA	272 DMPE	11734 H_2O 42 K^+ 32 Cl-	1 x 500
OmpC trimer MlaA (ClusPro model)	980 DMPE	36113 H_2O 98 K^+ 98 Cl^-	1 x 500 1 x 320 1 x 130

In total, three separate production simulations with different initial velocities were performed of the OmpC-MlaA complex, resulting in 3 trajectories of 500 ns, 320 ns, and 130 ns in length, respectively. Clustering was performed on the MlaA structures obtained from a combined trajectory of all three atomistic simulations – a total of 4750 frames spaced every 0.2 ns. The structures were assigned to clusters using Root Mean Squared Distance (RMSD) with a 0.1 nm cut-off. Four clusters were observed to contain greater than 100 frames. The central structure of these four clusters was used to generate MlaA parameters for four separate Coarse Grained simulations. trj_cavity was used to identify the location the pore cavity (19), and Hole was used to create the pore profile (20).

Coarse Grained Simulations. In total, 6 Coarse Grained (CG) simulations were performed (Table B). The CG simulations were performed using the MARTINI 2.2 force field (21, 22). An elastic network was used to preserve the tertiary and quaternary structures of proteins. The network was created between backbone beads that were within a range of 0.5 and 0.9 nm from one another in the initial structure. The harmonic potential force constant for elastic bonds was set to 500 kJ mol^{-1} nm^{-2}. The elastic network was applied separately to the OmpC trimeric complex and MlaA i.e. there were no harmonic bonds between the OmpC trimer and MlaA.

In all simulations, the equations of motion were integrated using the Verlet leapfrog algorithm with a step size of 10 fs. Electrostactic interactions were treated using the reaction field method with a short-range cutoff of 1.1 nm (23). The dielectric constant was set to 15 within this cutoff. The van der Waals interactions were shifted to zero at 1.1 nm. The velocity rescale thermostat (24) was used to maintain a temperature of 323 K or 350 K and Berendsen barostat (25), with semi-isotropic coupling, was used to maintain a system pressure of 1 bar. Protein, membrane and solvent (water and ions) were coupled to separate thermostats. Initial velocities were set according to the Maxwell distribution.

The proteins were inserted into pre-equilibrated lipid bilayers, consisting of an asymmetric distribution of lipid A, 1-palmitoyl-2-vacenoyl-phosphatidylethanolamine (PVPE), and 1-palmitoyl-2-vacenoyl-

phosphatidylglycerol (PVPG), by superimposition of the protein and membrane coordinates. Any overlapping lipids and solvent particles were removed from the system. Any remaining bad contacts were relaxed with 1000 steps steepest decent energy minimization. Harmonic position restraints with a force constant of 1000 kJ mol^{-1} were placed on all protein backbone particles for 200 ns to allow the solvent and lipids to equilibrate around the proteins. The restraints were removed for production runs.

Table B. Summary of Coarse Grained Simulations: system components and simulations time.

Protein Configuration	Outer Leaflet Lipids	Inner Leaflet Lipids	Water and Ions	System Temp. (K)	Simulation time (# of simulations x ns)
OmpC trimer	58 lipid A 146 PVPE 16 PVPG	236 PVPE 25 PVPG	13887 W (10% WF) 116 Mg^{2+} 314 Na^{+} 228 Cl^{-}	350	1 x 8000
OmpC trimer MlaA (ClustPro model)	76 lipid A 69 PVPE 7 PVPG	198 PVPE 22 PVPG	6843 W (10% WF) 152 Mg^{2+} 692 Na^{+} 608 Cl^{-}	323	1 x 5000
OmpC trimer MlaA (Clusters 1 to 4 from all atom simulations)	76 lipid A 69 PVPE 7 PVPG	193 PVPE 22 PVPG	6800 W (10% WF) 152 Mg^{2+} 692 Na^{+} 608 Cl^{-}	323	4 x 5000

Backmapping protocol. CG coordinates were backmapped by the use of geometric projection and further force-field, CHARMM36 (12), relaxation (SD minimization). This was followed by a NVT equilibration simulation step, with position restraints placed on the heavy atoms of the protein, as described elsewhere (26).

Temperature titration for chromosomal *ompC* mutants. Purified wild-type and mutant OmpC-MlaA-His complexes were aliquoted into 1.5 mL centrifuge tubes and incubated in water bath set at different temperatures

for 10 min. 20 µl of each sample were transferred into separate tubes and mixed immediately with equal volume of 2 X Laemmlli buffer and subjected to SDS-PAGE in 12 % Tris.HCl gels, followed by Coomassie Blue staining (Sigma-Aldrich).

LPS labeling and lipid A isolation. Mild acid hydrolysis of [^{32}P]-labeled cultures was used to isolate lipid A according to a procedure described previously (1, 27, 28) with some modifications. 5 mL cultures were grown (inoculated with overnight cultures at 1:100 dilution) in LB broth at 37 °C until OD_{600} reached ~0.5–0.7 (exponential) or ~2–4 (stationary). Cultures were uniformly labeled with 1 µCi mL−1 [^{32}P]-disodium phosphate (Perkin-Elmer) from the start of inoculation. One MC4100 wild-type culture labeled with [^{32}P] was treated with 25 mM EDTA, pH 8.0 for 10 min prior to harvesting. Cells (5 mL and 1 mL for exponential and stationary phase cultures respectively) were harvested by centrifugation at 4700 × *g* for 10 min and washed twice with 1 mL PBS (137 mM NaCl, 2.7 mM KCl, 10 mM Na_2HPO_4, 1.8 mM KH_2PO_4, pH 7.4) at 5000 × *g* for 10 min. Each cell pellet was resuspended in 0.32 mL PBS, and converted into single phase Bligh/Dyer mixture (chloroform/methanol/water:1/2/0.8) by adding 0.8 mL methanol and 0.4 mL chloroform. The single phase Bligh/Dyer mixture was incubated at room temperature for 20 min, followed by centrifugation at 21,000 × *g* for 30 min. Each pellet obtained was washed once with 1 mL freshly made single phase Bligh/Dyer mixture and centrifuged as above. The pellet was later resuspended in 0.45 mL 12.5 mM sodium acetate containing 1 % SDS, pH 4.5. The mixture was sonicated for 15 min before incubation at 100 °C for 40 min. The mixture was converted to a two-phase Bligh/Dyer mixture (chloroform/methanol/water: 2/2/1.8) by adding 0.50 mL methanol and 0.50 mL chloroform. The lower phase of each mixture was collected after phase partitioning by centrifugation at 21 000 × *g* for 30 min. The collected lower phase was washed once with 1 mL of the upper phase derived from the freshly made two-phase Bligh/Dyer mixture and centrifuged as above. The final lower phase was collected after phase partitioning by centrifugation and dried under N_2 gas. The dried radiolabeled lipid A samples were redissolved in 100 µL of chloroform/methanol mixture (4/1), and 20 µL of the samples were used for scintillation counting (MicroBeta2®, Perkin-Elmer). Equal amounts of radiolabeled lipids (cpm/lane) were spotted onto the TLC plate (Silica Gel 60 F254, Merck Millipore) and

were separated using the solvent system consisting of chloroform/pyridine/96 % formic acid/water (50/50/14.6/4.6) (29). The TLC plate was then dried and exposed to phosphor storage screens (GE Healthcare). Phosphor-screens were visualized in a phosphor-imager (Storm 860, GE Healthcare), and the spots were analyzed by ImageQuant TL analysis software (version 7.0, GE Healthcare). Spots were quantified and averaged based on three independent experiments of lipid A isolation.

OM permeability studies. OM sensitivity against SDS/EDTA was judged by colony-forming-unit (CFU) analyses on LB agar plates containing indicated concentrations of SDS/EDTA. Briefly, 5 mL cultures were grown (inoculated with overnight cultures at 1:100 dilution) in LB broth at 37 °C until OD_{600} reached ~0.4-0.6. Cells were normalized by optical density, first diluted to OD_{600} = 0.1 (~10^8 cells), and then serially diluted (ten-fold) in LB broth using 96-well microtiter plates. 2.5 µL of the diluted cultures were manually spotted onto the plates, dried, and incubated overnight at 37 °C. Plate images were visualized by *G*:Box Chemi-XT4 (Genesys version 1.4.3.0, Syngene).

SDS-PAGE, immunoblotting and staining. All samples subjected to SDS-PAGE were mixed 1:1 with 2X Laemmli buffer. Except for temperature titration experiments, the samples were subsequently either kept at room temperature or subjected to boiling at 100 °C for 10 min. Equal volumes of the samples were loaded onto the gels. As indicated in the figure legends, SDS-PAGE was performed using either 12% or 15% Tris.HCl gels (30) or 15% Tricine gel (31) at 200 V for 50 min. After SDS-PAGE, gels were visualized by either Coomassie Blue staining, or subjected to immunoblot analysis. Immunoblot analysis was performed by transferring protein bands from the gels onto polyvinylidene fluoride (PVDF) membranes (Immun-Blot 0.2 µm, Bio-Rad, CA, USA) using semi-dry electroblotting system (Trans-Blot Turbo Transfer System, Bio-Rad). Membranes were blocked for 1 h at room temperature by 1 X casein blocking buffer (Sigma-Aldrich), washed and incubated with either primary antibodies (monoclonal α-MlaA (1) (1:3000) and α-OmpC (2) (1:1500)) or monoclonal α-His

antibody (pentahistidine) conjugated to the horseradish peroxidase (HRP) (Qiagen, Hilden, Germany) at 1:5000 dilution for 1 – 3 h at room temperature. Secondary antibody ECL™ anti-mouse IgG-HRP was used at 1:5000 dilution. Luminata Forte Western HRP Substrate (Merck Millipore) was used to develop the membranes, and chemiluminescence signals were visualized by *G*:Box Chemi-XT4 (Genesys version 1.4.3.0, Syngene).

Supplementary references

1. Chong ZS, Woo WF, & Chng SS (2015) Osmoporin OmpC forms a complex with MlaA to maintain outer membrane lipid asymmetry in Escherichia coli. *Mol Microbiol* 98(6):1133-1146.
2. Khetrapal V, *et al.* (2015) A set of powerful negative selection systems for unmodified Enterobacteriaceae. *Nucleic Acids Res* 43(13):e83.
3. Murphy KC & Campellone KG (2003) Lambda Red-mediated recombinogenic engineering of enterohemorrhagic and enteropathogenic E. coli. *BMC Mol Biol* 4:11.
4. Chin JW, Martin AB, King DS, Wang L, & Schultz PG (2002) Addition of a photocrosslinking amino acid to the genetic code of Escherichiacoli. *Proc Natl Acad Sci U S A* 99(17):11020-11024.
5. Ryu Y & Schultz PG (2006) Efficient incorporation of unnatural amino acids into proteins in Escherichia coli. *Nat Methods* 3(4):263-265.
6. Slotboom DJ, Duurkens RH, Olieman K, & Erkens GB (2008) Static light scattering to characterize membrane proteins in detergent solution. *Methods* 46(2):73-82.
7. Kozakov D, *et al.* (2017) The ClusPro web server for protein-protein docking. *Nat Protoc* 12(2):255-278.
8. Ovchinnikov S, *et al.* (2017) Protein structure determination using metagenome sequence data. *Science* 355(6322):294-298.
9. Basle A, Rummel G, Storici P, Rosenbusch JP, & Schirmer T (2006) Crystal structure of osmoporin OmpC from E. coli at 2.0 A. *J Mol Biol* 362(5):933-942.

10. Berendsen HJC vdSD, van Drunen R (1995) GROMACS: A message-passing parallel molecular dynamics implementation. . *Comput Phys Commun* 91(1-3):43-56.

11. Van Der Spoel D, *et al.* (2005) GROMACS: fast, flexible, and free. *J Comput Chem* 26(16):1701-1718.

12. Best RB, *et al.* (2012) Optimization of the additive CHARMM all-atom protein force field targeting improved sampling of the backbone phi, psi and side-chain chi(1) and chi(2) dihedral angles. *J Chem Theory Comput* 8(9):3257-3273.

13. Hess B BH, Berendsen HJC, Fraaije JGEM (1997) LINCS: A linear constraint solver for molecular simulations. *J Comput Chem* 18(12):8577-8593.

14. Essmann U, *et al.* (1995) A smooth particle mesh Ewald method. *The Journal of Chemical Physics* 103(19):8577-8593.

15. NosÉ S (2002) A molecular dynamics method for simulations in the canonical ensemble. *Molecular Physics* 100(1):191-198.

16. Hoover WG (1985) Canonical dynamics: Equilibrium phase-space distributions. *Phys Rev A Gen Phys* 31(3):1695-1697.

17. Nosé S & Klein ML (2006) Constant pressure molecular dynamics for molecular systems. *Molecular Physics* 50(5):1055-1076.

18. Wolf MG, Hoefling M, Aponte-Santamaria C, Grubmuller H, & Groenhof G (2010) g_membed: Efficient insertion of a membrane protein into an equilibrated lipid bilayer with minimal perturbation. *J Comput Chem* 31(11):2169-2174.

19. Paramo T, East A, Garzon D, Ulmschneider MB, & Bond PJ (2014) Efficient Characterization of Protein Cavities within Molecular Simulation Trajectories: trj_cavity. *J Chem Theory Comput* 10(5):2151-2164.

20. Smart OS, Goodfellow JM, & Wallace BA (1993) The pore dimensions of gramicidin A. *Biophys J* 65(6):2455-2460.

21. Monticelli L, *et al.* (2008) The MARTINI Coarse-Grained Force Field: Extension to Proteins. *J Chem Theory Comput* 4(5):819-834.

22. Marrink SJ, Risselada HJ, Yefimov S, Tieleman DP, & de Vries AH (2007) The MARTINI force field: coarse grained model for biomolecular simulations. *J Phys Chem B* 111(27):7812-7824.

23. Tironi IG, Sperb R, Smith PE, & van Gunsteren WF (1995) A generalized reaction field method for molecular dynamics simulations. *The Journal of Chemical Physics* 102(13):5451-5459.

24. Bussi G, Donadio D, & Parrinello M (2007) Canonical sampling through velocity rescaling. *J Chem Phys* 126(1):014101.

25. Berendsen HJC, Postma JPM, van Gunsteren WF, DiNola A, & Haak JR (1984) Molecular dynamics with coupling to an external bath. *The Journal of Chemical Physics* 81(8):3684-3690.

26. Wassenaar TA, Pluhackova K, Bockmann RA, Marrink SJ, & Tieleman DP (2014) Going Backward: A Flexible Geometric Approach to Reverse Transformation from Coarse Grained to Atomistic Models. *J Chem Theory Comput* 10(2):676-690.

27. Zhou Z, Lin S, Cotter RJ, & Raetz CR (1999) Lipid A modifications characteristic of Salmonella typhimurium are induced by NH4VO3 in Escherichia coli K12. Detection of 4-amino-4-deoxy-L-arabinose, phosphoethanolamine and palmitate. *J Biol Chem* 274(26):18503-18514.

28. Jia W, *et al.* (2004) Lipid trafficking controls endotoxin acylation in outer membranes of Escherichia coli. *J Biol Chem* 279(43):44966-44975.

29. Wu T, *et al.* (2006) Identification of a protein complex that assembles lipopolysaccharide in the outer membrane of Escherichia coli. *Proc Natl Acad Sci U S A* 103(31):11754-11759.

30. Laemmli UK (1970) Cleavage of structural proteins during the assembly of the head of bacteriophage T4. *Nature* 227(5259):680-685.

31. Schagger H (2006) Tricine-SDS-PAGE. *Nat Protoc* 1(1):16-22.

32. Kyte J & Doolittle RF (1982) A simple method for displaying the hydropathic character of a protein. *J Mol Biol* 157(1):105-132.

33. Casadaban MJ (1976) Transposition and fusion of the lac genes to selected promoters in Escherichia coli using bacteriophage lambda and Mu. *J Mol Biol* 104(3):541-555.

34. Ruiz N, Chng SS, Hiniker A, Kahne D, & Silhavy TJ (2010) Nonconsecutive disulfide bond formation in an essential integral outer membrane protein. *Proc Natl Acad Sci U S A* 107(27):12245-12250.

35. Chang AC & Cohen SN (1978) Construction and characterization of amplifiable multicopy DNA cloning vehicles derived from the P15A cryptic miniplasmid. *J Bacteriol* 134(3):1141-1156.

36. Weiss DS, Chen JC, Ghigo JM, Boyd D, & Beckwith J (1999) Localization of FtsI (PBP3) to the septal ring requires its membrane anchor, the Z ring, FtsA, FtsQ, and FtsL. *J Bacteriol* 181(2):508-520.

Supplementary Figures

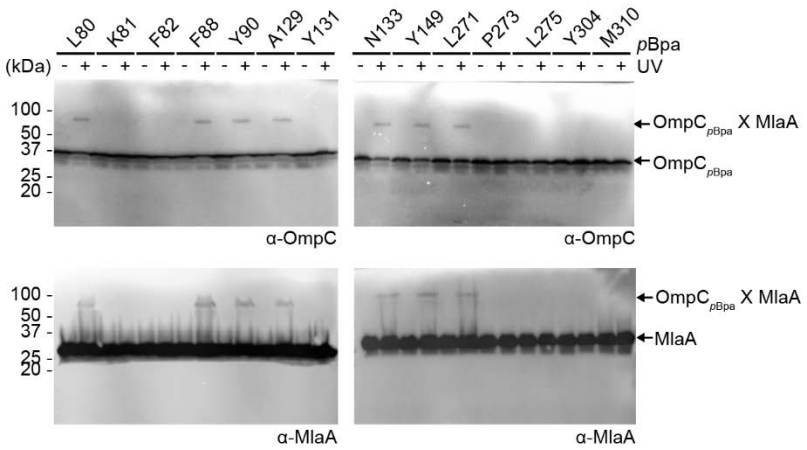

Figure S1. Seven more positions at the dimeric interface of the OmpC trimer contact MlaA. Immunoblots showing UV-dependent formation of crosslinks between OmpC and MlaA in Δ*ompC* cells expressing OmpC substituted with *p*Bpa at indicated positions, selected as part of the localized search.

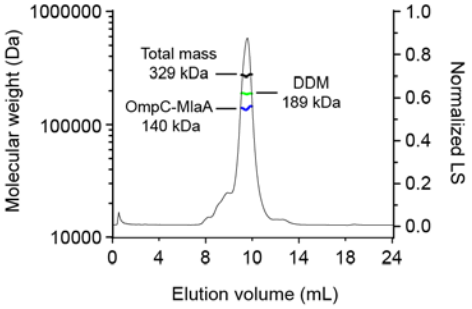

Figure S2. SEC-MALS analysis of the OmpC-MlaA complex revealing that one copy of MlaA binds to the OmpC trimer. As indicated, total molecular mass: 329 (± 0.4%) kDa; protein molecular mass: 140 (± 0.4%) kDa (observed), 148 kDa (predicted, $OmpC_3MlaA$); modifier (DDM) molecular mass: 189 (± 0.8%) kDa. Numbers stated after ± show statistical consistency of analysis.

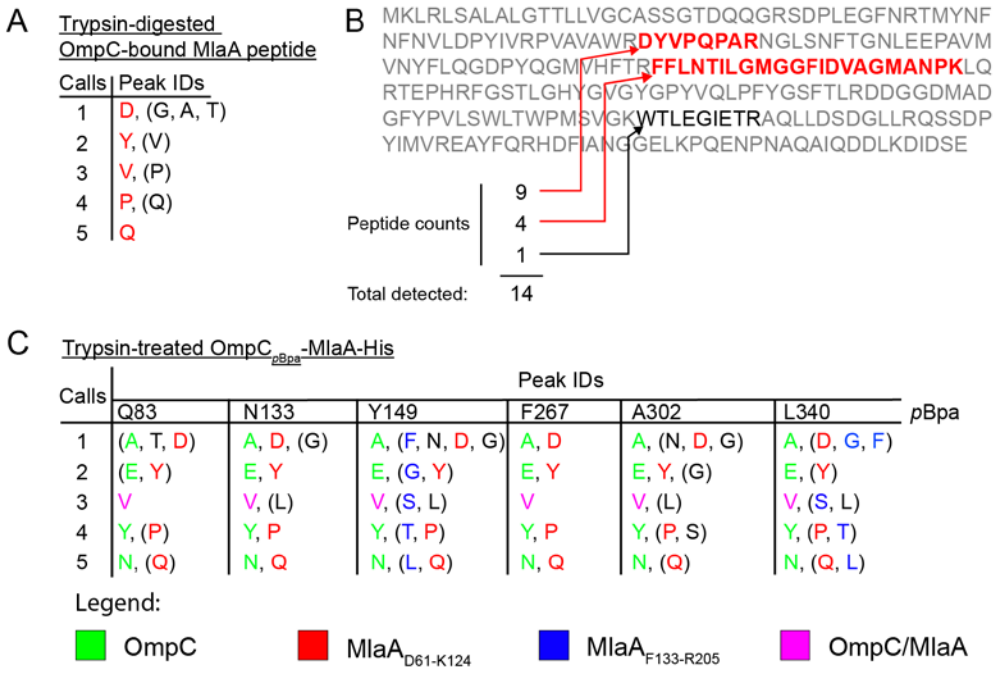

Figure S3. N-terminal sequencing and MS/MS analyses identified two specific MlaA peptides binding to OmpC. (*A*) First five residue calls for the MlaA peptide remaining bound to OmpC after trypsin digestion (see Fig. 2*A*) revealed that it starts with D^{61}YVPQ of full-length MlaA protein. (*B*) MS/MS analysis of the MlaA peptide remaining bound to OmpC after trypsin digestion detected two MlaA fragments with high peptide counts (sequences colored *red*), suggesting that the OmpC-bound peptide has boundaries from D61 to K124. (*C*) First five residue calls for protein bands containing MlaA peptides crosslinked to $OmpC_{pBpa}$ (see Fig. 2*B*) revealed the presence of MlaA peptides starting with D^{61}YVPQ and F^{133}GSTL, along with OmpC N-terminus A^{21}EVYN. Residue calls are assigned to the respective protein/peptide as denoted by the legend.

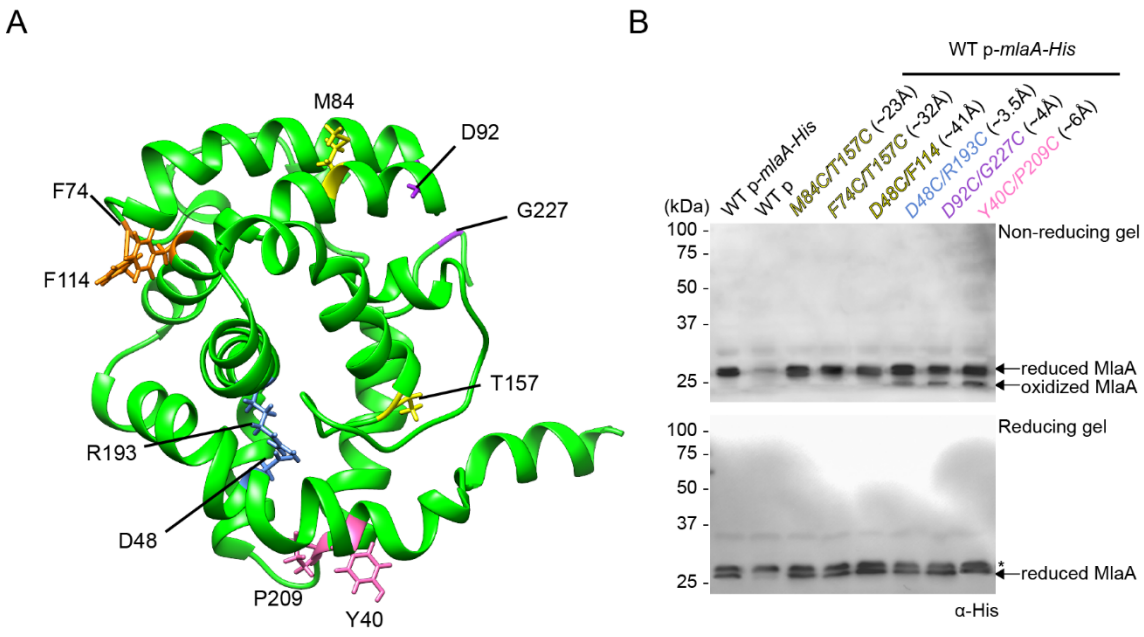

Figure S4. Residue pairs on MlaA predicted to contact each other based on coevolution analysis allow the formation of disulfide bonds when substituted with cysteines. (*A*) Cartoon representation of the MlaA structural model predicted based on residue-residue contacts inferred from coevolution analysis of metagenomic sequence data prediction (GREMLIN, (8)), with strongly co-evolved residue pairs that are mutated to cysteines highlighted (same colored sticks). (*B*) Immunoblots showing oxidized or reduced forms of indicated MlaA-His double cysteine variants expressed in wild-type cells from the pET23/42 vector (p). Samples were subjected to non-reducing (*top*) or reducing (*bottom*) SDS-PAGE prior to transfer. A protein that cross-reacted with the α-His antibody is denoted with (*). Distances between cysteine pairs in unit angstrom (Å), as measured in the model in (*A*), are indicated in parentheses.

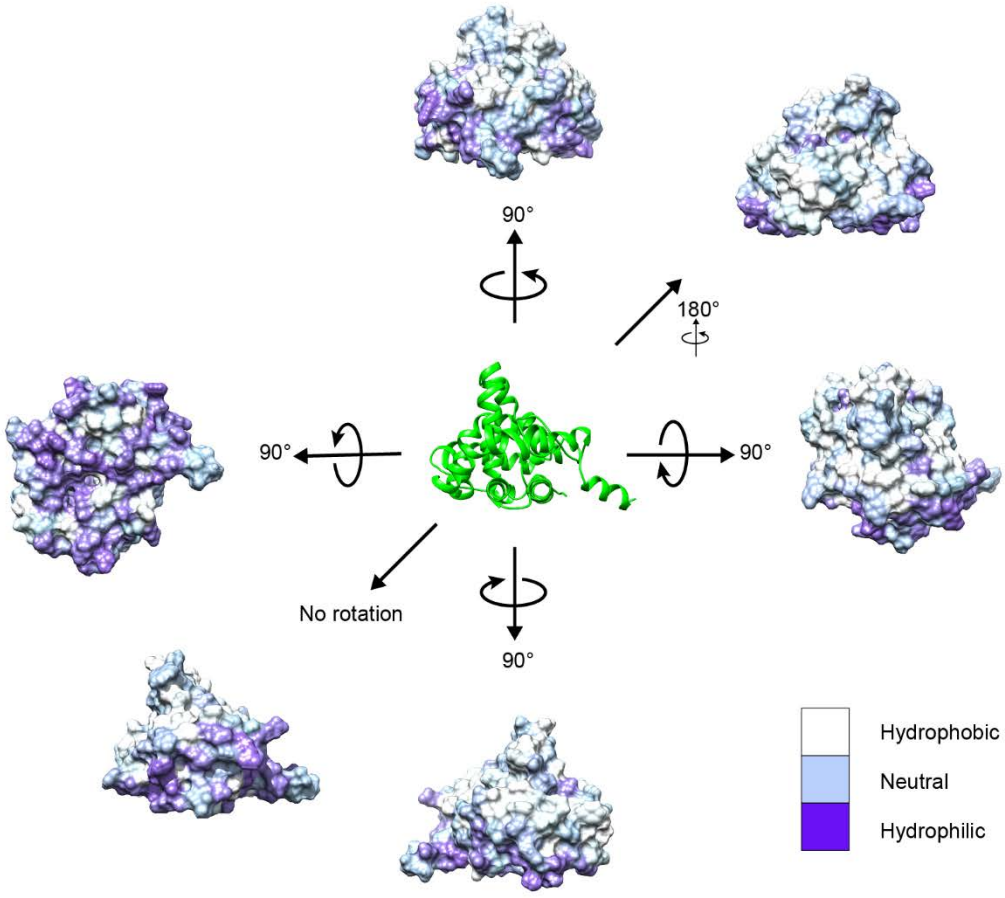

Figure S5. The surface of MlaA is mostly hydrophobic. Surface representation of the MlaA model (8) depicted in multiple orientations and colored based on amino acid hydrophobicity. Purple, light blue and white represent most hydrophilic to most hydrophobic amino acids based on the Kyte-Doolittle scale (32).

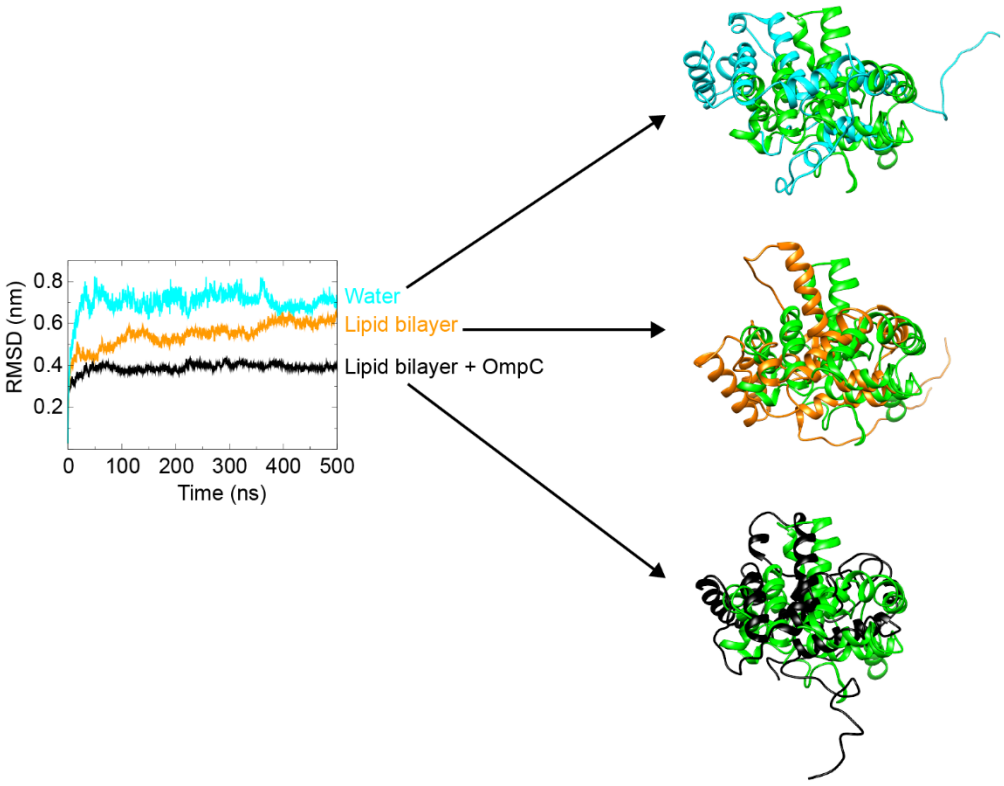

Figure S6. The MlaA structure modelled from co-evolution analysis (8) is most stable in the lipid bilayer and when bound to OmpC. Averaged root-mean-square-deviation (RMSD) plots illustrating the changes of the backbone of MlaA models over the course of all-atomistic MD simulations when placed in water (*cyan*), a lipid bilayer (*orange*), or in complex with OmpC in the bilayer (*black*). Superimpositions of the initial (*green*) and final structures for each simulation are shown on the right.

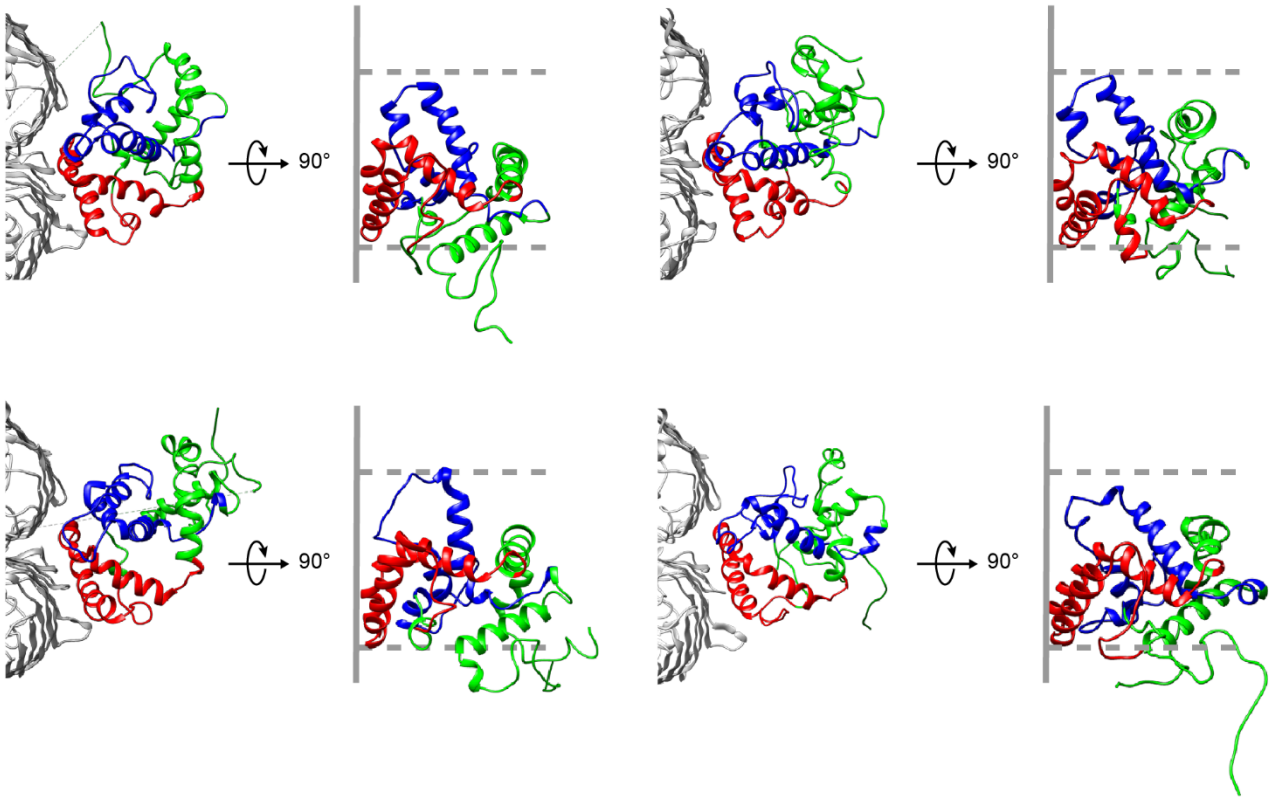

Figure S7. Four major clusters of all-atomistic MD simulated OmpC-MlaA structure depict how MlaA interacts with OmpC in the OM bilayer. The bottom right model is reproduced in Fig. 3*A*. $MlaA_{D61\text{-}K124}$ and $MlaA_{F133\text{-}R205}$ peptides are highlighted in *red* and *blue*, respectively, as in Fig. 2*D*. The OM boundaries are indicated as gray dashed lines.

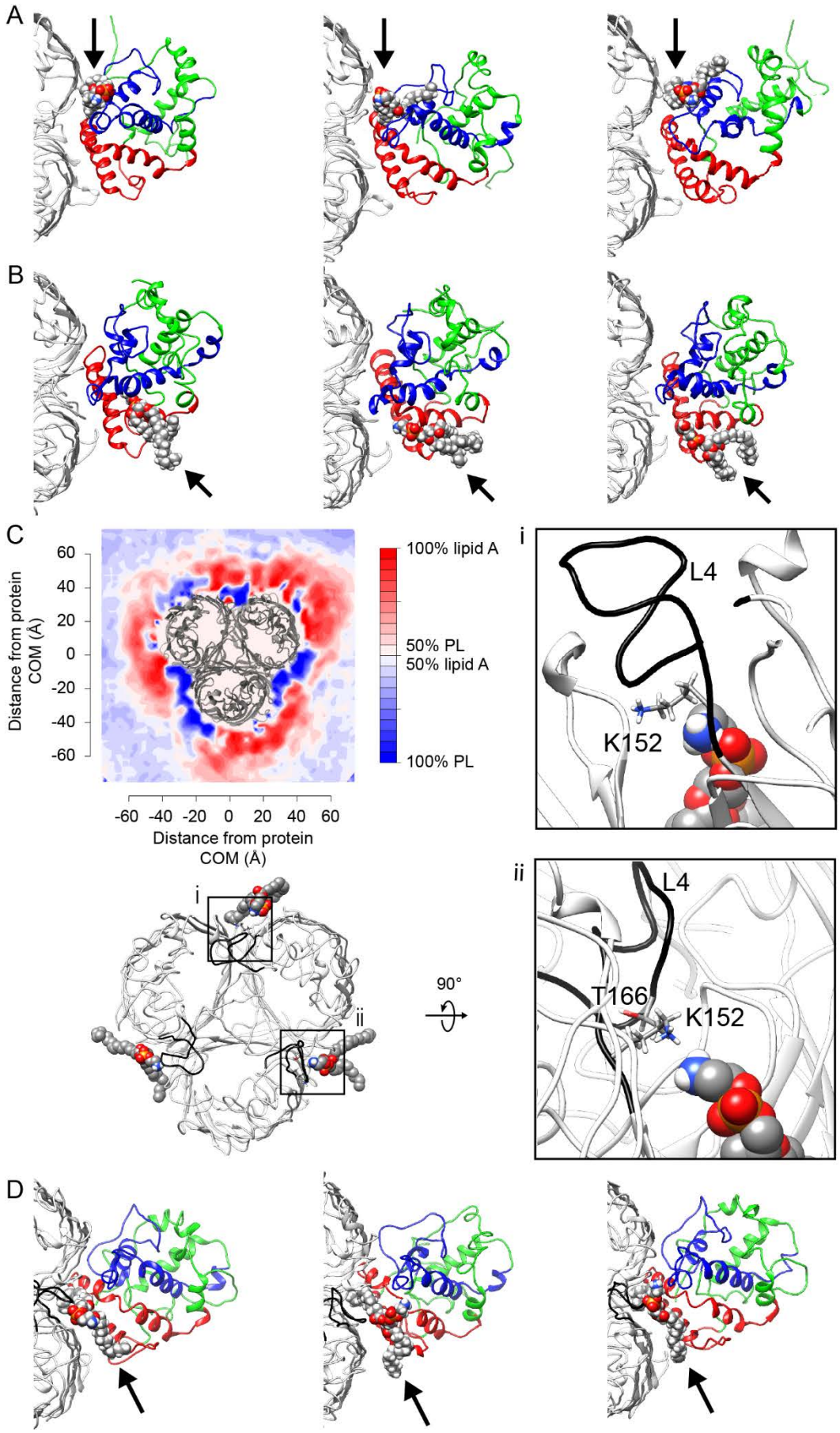
A
B
C
60
40
20
0
-20
-40
-60
Distance from protein COM (Å)
-60 -40 -20 0 20 40 60
Distance from protein COM (Å)
100% lipid A
50% PL
50% lipid A
100% PL
i
ii
90°
L4
K152
L4
T166
K152
D

Figure S8. Snapshots of MD simulations depicting PLs found around the OmpC-MlaA complex. (*A*) Cartoon representations (*top view*) of OmpC-MlaA structural models backmapped from coarse-grained simulations depicting PL molecules (*spheres*) found at the binding interfaces between OmpC (*white*) and MlaA (overall *green*, but with $MlaA_{D61\text{-}K124}$ and $MlaA_{F133\text{-}R205}$ peptides highlighted in *red* and *blue*, respectively, as in Fig. 2*D*). (*B*) Cartoon representations (*top view*) of OmpC-MlaA structural models backmapped from coarse-grained simulations highlighting PL molecules (*spheres*) approaching the putative channel of MlaA via their headgroups. (*C*) Contour map indicating relative probability of finding outer leaflet PLs and lipid A around an OmpC trimer (cartoon representation, *top view*) in an asymmetric OM bilayer model. The outer leaflet of the OM contains PLs and lipid A in a 3:1 molar ratio. Cartoon representation (*top view*) of OmpC (*white*) with PLs (*spheres*) found at the dimeric interfaces is shown below. Residues in loop 4 of OmpC ($L4_{OmpC}$, *black*) interacting with the PL headgroups are highlighted in the expanded representations on the right (*i* and *ii*). (*D*) Cartoon representations (*top view*) of OmpC-MlaA structural models backmapped from coarse-grained simulations depicting PLs (*spheres*) found between OmpC and MlaA.

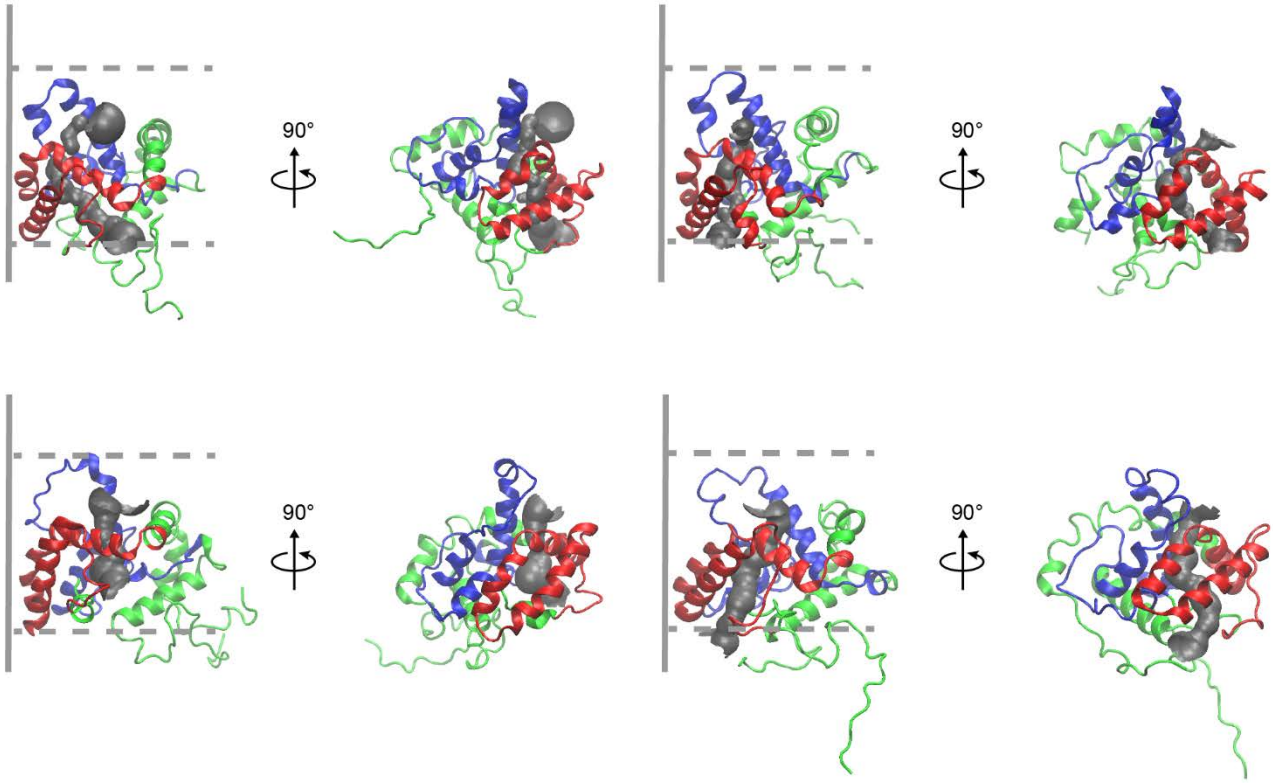

Figure S9. Four major clusters of all-atomistic MD simulated OmpC-MlaA structure with the putative channels depicted in *gray*. The bottom right model is reproduced in Fig. 4*A*. OmpC is represented as gray solid lines. $MlaA_{D61\text{-}K124}$ and $MlaA_{F133\text{-}R205}$ peptides are highlighted in *red* and *blue*, respectively, as in Fig. 2*D*. The OM boundaries are indicated as gray dashed lines.

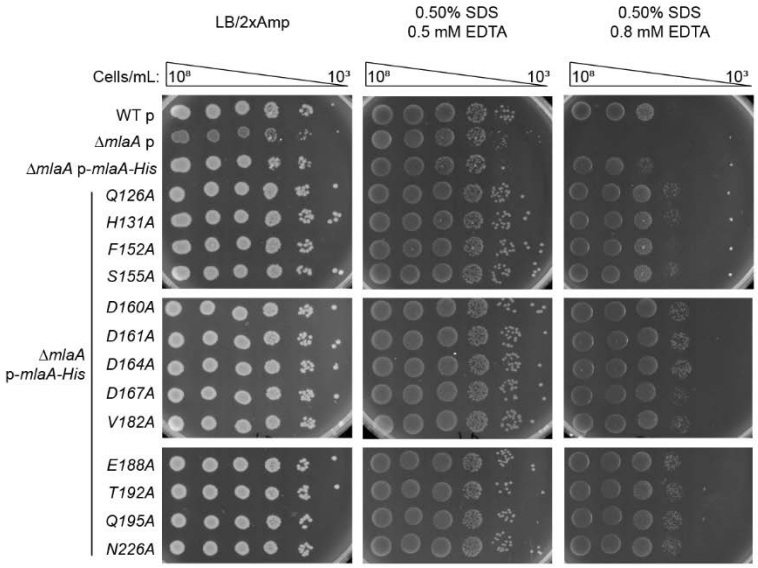

Figure S10. Single alanine substitutions in the putative channel do not disrupt the function of MlaA. Analysis of SDS/EDTA sensitivity of wild-type (WT) and Δ*mlaA* strains producing indicated MlaA channel variants from the pET23/42 vector (p).

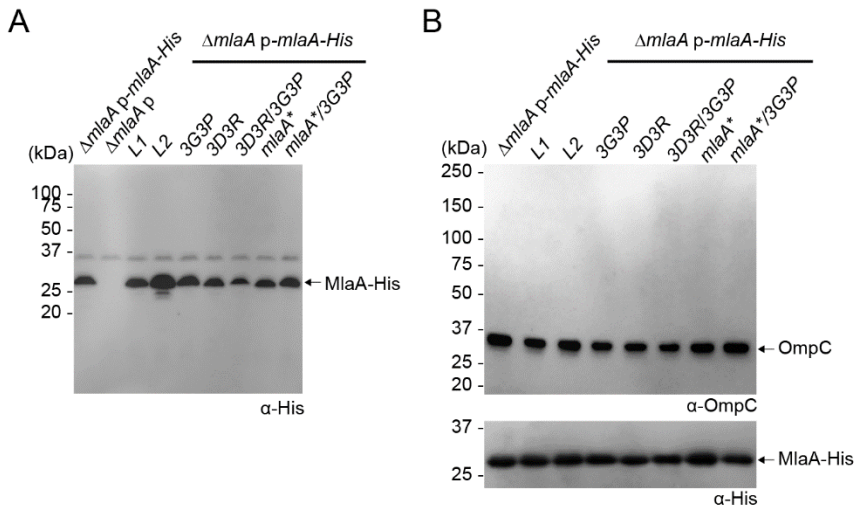

Figure S11. Mutations in functional regions of MlaA do not significantly affect protein levels or its interaction with OmpC. (*A*) Immunoblot showing the levels of indicated MlaA-His variants produced from the pET23/42 vector (p) in the Δ*mlaA* strain. (*B*) Immunoblots showing OmpC copurified with indicated MlaA-His variants produced from the pET23/42 vector (p) in the Δ*mlaA* strain.

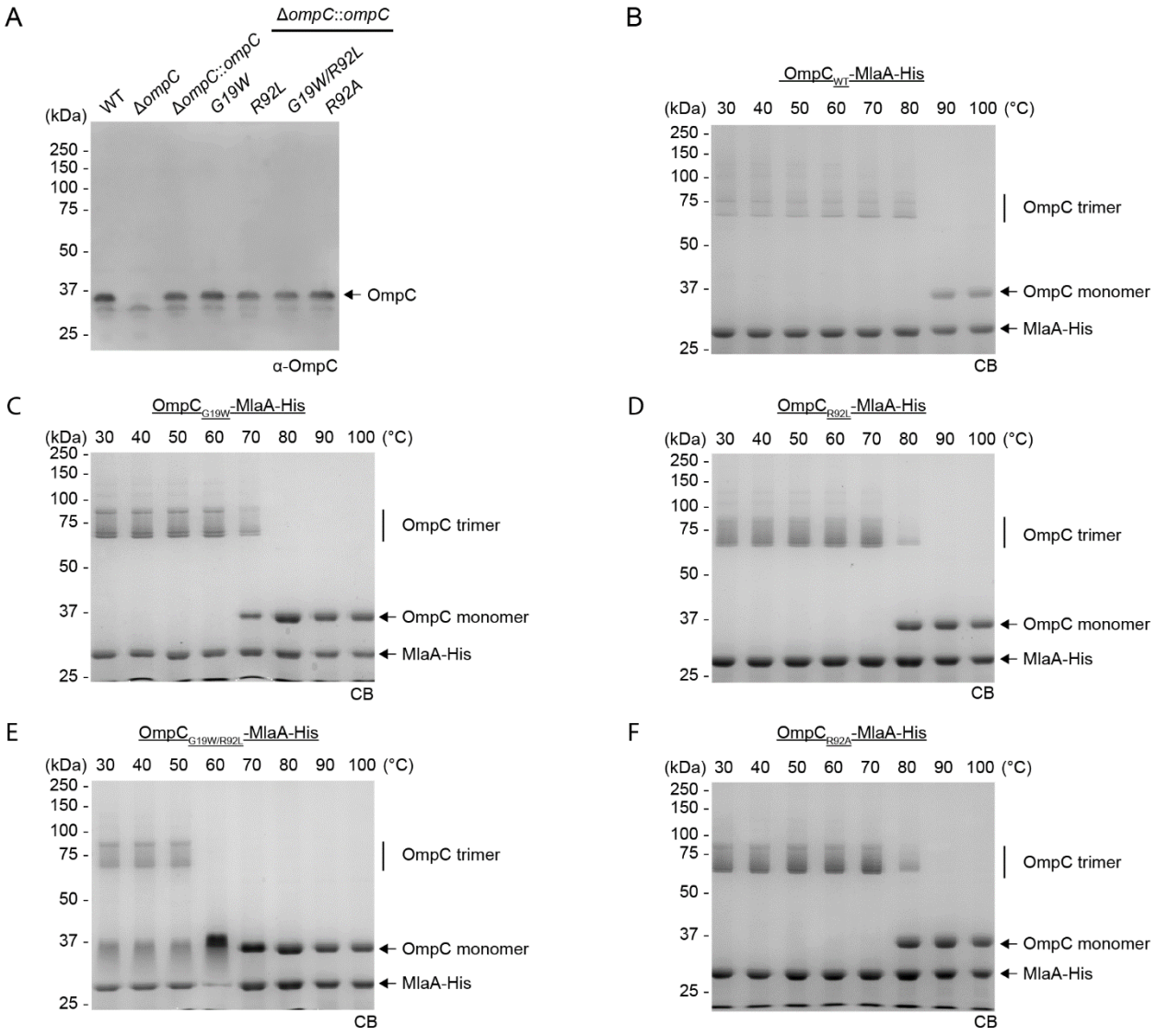

Figure S12. Mutations on residues G19 and R92 do not affect OmpC levels in cells, but weaken trimer stability in vitro. (*A*) Immunoblot showing the levels of wild-type OmpC and indicated OmpC variants produced from the chromosomal locus. (*B-F*) In vitro temperature titration of purified OmpC-MlaA-His and the indicated variants subjected to seminative SDS-PAGE (12% Tris.HCl gel), followed by Coomassie blue (CB) staining.

Supplementary Tables

Table S1. Bacterial strains used in this study

Strains	Relevant genotypes and characteristics	References
MC4100	*F- araD139 Δ(argF-lac) U169 rpsL150 relA1 flbB5301 ptsF25 deoC1 ptsF25 thi*	(33)
NovaBlue	*endA1 hsdR17 (rK12– mK12+) supE44 thi-1 recA1 gyrA96 relA1 lac F' [proA+ B+ lacIq ZΔM15*::*Tn10]*	Novagen
BL21(λDE3)	*fhuA2 [lon] ompT gal (λDE3) [dcm] ΔhsdS λDE3 = λ sBamHIo ΔEcoRI-B int*::*(lacI*::*PlacUV5*::*T7 gene1) i21 Δnin5*	Novagen
TKW001	BL21(λDE3) Δ*ompF*::*kan*	This study
CZS010	MC4100 Δ*mlaA*::*kan*	(1)
CZS015	MC4100 Δ*ompC*::*kan*	(1)
NR1216	MC4100 Δ*dsbA*::*kan*	(34)

Table S2. Plasmids used in this study

Plasmids	Relevant genotypes and characteristics	References
pET22b(+)	pT7lac inducible expression vector, contains N-terminal PelB signal peptide for periplasmic localization; Amp^R	Novagen
pET23/42	pT7 inducible expression vector, contains multiple cloning site of pET42a(+) in pET23a(+) backbone; Amp^R	(29)
pSLC-246	Template plasmid encoding kanamycin resistance gene for positive selection and toxin gene (*tse2*) under the control of rhamnose induceable promoter (P_{rhaB}) for negative selection.	(2)
pSup-BpaRS-6TRN	Encodes an orthogonal tRNA and aminoacyl-tRNA synthetase permitting ribosomal incorporation of *p*Bpa at TAG stop codons	(5)
pKM208	A variation of pKM201 expresses the *lacI* repressor gene that keep expression of *red* and *gam* under tight control prior to IPTG induction	(3)
pACYC184	Low copy cloning vector; Cam^R	(35)
pCDFDuet-1	pT7 inducible expression vector; $Spec^R$	Novagen
pDSW206	Promoter down mutations in -35 and -10 of pTrc99a; Amp^R	(36)
pET23/42*mlaA-His*	Encodes full length MlaA with C-terminal His8 tag; Amp^R (p-*mlaA-His*)	(1)
pCDF*mlaA-His*	Encodes full length MlaA with C-terminal His8 tag; $Spec^R$	This study
pCDF-*dmlaA-His*	Encodes delipidated version of MlaA (a.a. 19-250) with N-terminal PelB signal peptide (for periplasmic localization) and C-terminal His8 tag; $Spec^R$	This study
pET22b(+)*dmlaA-His*	Encodes delipidated version of MlaA (a.a. 19-250) with N-terminal PelB signal peptide and C-terminal His6 tag; Amp^R	(1)
pACYC184*ompC*	Encodes full length OmpC under its native promoter; Cam^R	(1)
pDSW206*ompC*	Encodes full length OmpC inducible by *lacI* promoter; Amp^R	This study

Table S3. Primers used in this study.

Primers	Sequence (5' to 3')*
ompC_A129B FP	GGTAACGGCTTCTAGACCTACCGTAACACTGAC
ompC_A129B RP	GTTACGGTAGGTCTAGAAGCCGTTACCACGCTG
ompC_A302B FP	GTTGATGTTGGTTAGACCTACTACTTCAACAAAAACATGTCC
ompC_A302B RP	GAAGTAGTAGGTCTAACCAACATCAACATATTTCAGGATATC
ompC_D7B FP	GAAGTTTACAACAAATAGGGCAACAAATTAGATCTGTACGG
ompC_D7B RP	GATCTAATTTGTTGCCCTATTTGTTGTAAACTTCAGCAGCG
ompC_F267B FP	GCTCAGTACCAGTAGGACTTCGGTCTGCGTCCG
ompC_F267B RP	CAGACCGAAGTCCTACTGGTACTGAGCAACAGC
ompC_F40B FP	CCTACATGCGTCTTGGCTAGAAAGGTGAAACTCAGG
ompC_F40B RP	GTTTCACCTTTCTAGCCAAGACGCATGTAGGTCTGG
ompC_F82B FP	GGCATTCGCAGGTCTGAAATAGCAGGATGTGGGTTC
ompC_F82B RP	GTCGAAAGAACCCACATCCTGCTATTTCAGACCTGC
ompC_F88B FP	GATGTGGGTTCTTAGGACTACGGTCGTAACTACGG
ompC_F88B RP	ACGACCGTAGTCCTAAGAACCCACATCCTG G
ompC_G138B FP	CACTGACTTCTTCTAGCTGGTTGACGGCCTGAACTTTGC
ompC_G138B RP	GGCCGTCAACCAGCTAGAAGAAGTCAGTGTTACGG
ompC_G151B FP	GTTCAGTACCAGTAGAAAAACGGCAACCCATCTGGTG
ompC_G151B RP	GTTGCCGTTTTTCTACTGGTACTGAACAGCAAAGTTC
ompC_G86B FP	TTC CAG GAT GTGTAGTCT TTC GAC TAC GGT CGT AAC
ompC_G86B RP	GTAGTCGAAAGACTACACATCCTGGAATTTCAGACCTGC
ompC_G8B FP	GAAGTTTACAACAAAGACTAGAACAAATTAGATCTGTACGG
ompC_G8B RP	GATCTAATTTGTTCTAGTCTTTGTTGTAAACTTAGCAGCG
ompC_K81B FP	CATTCGCAGGTCTGTAGTTCCAGGATGTGGGTTC
ompC_K81B RP	CACATCCTGGAACTACAGACCTGCGAATGCCACAC
ompC_L143B FP	CTGGTTGACGGCTAGAACTTTGCTGTTCAGTACC
ompC_L143B RP	CAGCAAAGTTCTAGCCGTCAACCAGACCGAAG
ompC_L271B FP	GTTCGACTTCGGTTAGCGTCCGTCCCTGGCTTAC
ompC_L271B RP	CAGGGACGGACGCTAACCGAAGTCGAACTGGTAC
ompC_L275B FP	GCGTCCGTCCTAGGCTTACCTGCAGTCTAAAG
ompC_L275B RP	GCAGGTAAGCCTAGGACGGACGCAGACCGAAG
ompC_L340B FP	AACATCGTAGCTTAGGGTCTGGTTTACCAGTTC
ompC_L340B RP	GTA AAC CAG ACCCTAAGC TAC GAT GTT ATC AGT GTT G
ompC_L50B FP	G GTT ACT GAC CAGTAGACC GGT TAC GGC CAG TG
ompC_L50B RP	GCC GTA ACC GGTCTACTG GTC AGT AAC CTG AGT TTC
ompC_L80B FP	GCA TTC GCA GGTTAGAAA TTC CAG GAT GTG GG
ompC_L80B RP	CATCCTGGAATTTCTAACCTGCGAATGCCACAC
ompC_M310B FP	CTTCAACAAAAACTAGTCCACCTACGTTGACTACAAAATC
ompC_M310B RP	CAACGTAGGTGGACTAGTTTTTGTTGAAGTAGTAGG
ompC_N133B FP	GCGACCTACCGTTAGACTGACTTCTTCGGTCTG
ompC_N133B RP	GAAGAAGTCAGTCTAACGGTAGGTCGCGAAGCC
ompC_P273B FP	CTTCGGTCTGCGTTAGTCCCTGGCTTACCTGCAG
ompC_P273B RP	GTAAGCCAGGGACTAACGCAGACCGAAGTCGAACTGG
ompC_Q266B FP	GTTGCTCAGTACTAGTTCGACTTCGGTCTGCGTC
ompC_Q266B RP	CCGAAGTCGAACTAGTACTGAGCAACAGCTTCG
ompC_Q83B FP	GGTCTGAAATTCTAGGATGTGGGTTCTTTCGAC

ompC_Q83B RP	AGAACCCACATCCTAGAATTTCAGACCTGCG
ompC_Y131B FP	CGGCTTCGCGACCTAGCGTAACACTGACTTCTTC
ompC_Y131B RP	GTCAGTGTTACGCTAGGTCGCGAAGCCGTTACC
ompC_Y149B FP	CTTTGCTGTTCAGTAGCAGGGTAAAAACGGCAAC
ompC_Y149B RP	GTTTTTACCCTGCTACTGAACAGCAAAGTTCAGGCCG
ompC_Y304B FP	GTTGGTGCTACCTAGTACTTCAACAAAAACATGTCC
ompC_Y304B RP	TTTGTTGAAGTACTAGGTAGCACCAACATCAACATATTTCAG
ompC_Y53B FP	CCAGCTGACCGGTTAGGGCCAGTGGGAATATC
ompC_Y53B RP	TCCCACTGGCCCTAACCGGTCAGCTGGTCAGTAAC
ompC_Y90B FP	GGTTCTTTCGACTAGGGTCGTAACTACGGCG
ompC_Y90B RP	GTAGTTACGACCCTAGTCGAAAGAACCCACATCCTG
ompC_NS_N5	ATGAAAGTTAAAGTACTGTCCCTCCTGGTCCCAGCTCTGCGTGTAG GCTGGAGCTGCTTC
ompC_NS_C3	TTAGAACTGGTAAACCAGACCCAGAGCTACGATGTTATCACATATG AA TATCCTCCTTAG
ompC_NS_N5_C	ATGAAAGTTAAAGTACTGTCCCTCCTG
ompC_NS_C3_C	TTAGAACTGGTAAACCAGACCCAG
mlaA_D160A FP	TTCACGCTGCGTGCGGACGGTGGTGATATGGCG
mlaA_D160A RP	ATCACCACCGTCCGCACGCAGCGTGAAGCTACC
mlaA_D161A FP	CGCTGCGTGATGCGGGTGGTGATATGGCGGATG
mlaA_D161A RP	CATATCACCACCCGCATCACGCAGCGTGAAGC
mlaA_D164A FP	GATGACGGTGGTGCGATGGCGGATGGTTTTTAC
mlaA_D164A RP	ACCATCCGCCATCGCACCACCGTCATCACGCAG
mlaA_D167A FP	GACGGTGGTGATATGGCGGCGGGTTTTTACCCG
mlaA_D167A RP	AAGAACCGGGTAAAAACCCGCCGCCATATCACC
mlaA_E188A FP	AAATGGACGCTTGCGGGGATCGAAACCCGCGC
mlaA_E188A RP	GTTTCGATCCCCGCAAGCGTCCATTTACCCAC
mlaA_F152A FP	GTTCAGTTACCGGCGTACGGTAGCTTCACGCTG
mlaA_F152A RP	GAAGCTACCGTACGCCGGTAACTGAACGTAAGG
mlaA_H131A FP	GGACTGAACCTGCGCGCTTCGGTAGTACGCTTG
mlaA_H131A RP	CTACCGAAGCGCGCAGGTTCAGTCCGTTGCAG
mlaA_N226A FP	GATTTCATCGCTGCGGGCGGCGAACTCAAACCG
mlaA_N226A RP	GAGTTCGCCGCCCGCAGCGATGAAATCATGACG
mlaA_Q126A FP	GAACCCGAAACTGGGCGCGGACTGAACCTCACCGC
mlaA_Q126A RP	GGTTCAGTCCGCGCCAGTTTCGGGTTCGCCATC
mlaA_Q195A FP	GAAACCCGCGCTGCGCTGCTGGATTCCGATGG
mlaA_Q195A RP	GAATCCAGCAGCGCAGCGCGGGTTTCGATCCC
mlaA_S155A FP	CCGTTCTACGGTGCGTTCACGCTGCGTGATGAC
mlaA_S155A RP	CGCAGCGTGAACGCACCGTAGAACGGTAACTG
mlaA_T192A FP	GAAGGGATCGAAGCGCGCGCTCAGCTGCTG
mlaA_T192A RP	CTGAGCGCGCGCGCTTCGATCCCTTCAAGCGTC
mlaA_V182A FP	GCCGATGTCTGCGGGTAAATGGACGCTTGAAG
mlaA_V182A RP	CGTCCATTTACCCGCAGACATCGGCCAGGTCAG
mlaA_D160R FP	TTCACGCTGCGTCGCGACGGTGGTGATATGGCG
mlaA_D160R RP	ATCACCACCGTCGCGACGCAGCGTGAAGCTACC

mlaA_D161R FP	CGCTGCGTGATCGCGGTGGTGATATGGCGGATG
mlaA_D161R RP	CATATCACCACCGCGATCACGCAGCGTGAAGC
mlaA_D164R FP	GATGACGGTGGTCGCATGGCGGATGGTTTTTAC
mlaA_D164R RP	ACCATCCGCCATGCGACCACCGTCATCACGCAG
mlaA_D167R FP	GACGGTGGTGATATGGCGCGCGGTTTTTACCCG
mlaA_D167R RP	AAGAACCGGGTAAAAACCGCGCGCCATATCACC
mlaA_D61R FP	GTCGCCTGGCGTCGCTATGTTCCGCAACCGGCG
mlaA_D61R RP	TTGCGGAACATAGCGACGCCAGGCGACAGCGAC
mlaA_E188R FP	AAATGGACGCTTCGCGGGATCGAAACCCGCGC
mlaA_E188R RP	GTTTCGATCCCGCGAAGCGTCCATTTACCCAC
3D3R FP SDM	CTTCACGCTGCGTCGCCGCGGTGGTCGC ATGGCGGATGGTTTTTACC
3D3R RP SDM	AACCATCCGCCATGCGACCACCGCGGCGACGCAGCGTGAAGCTACCG
F^{152}YGSF_to_5A FP	GTTCAGTTACCGGCGGCGGCGGCGGCGACGCTGCGTGATGACGGTGG
F^{152}YGSF_to_5A RP	CATCACGCAGCGTCGCCGCCGCCGCCGCCGGTAACTGAACGTAAGG
GVGYG_3G3A_FP	CTTGGTCATTATGCGGTGGCGTATGCGCCTTACGTTCAGTTACCG
GVGYG_3G3A_RP	CTGAACGTAAGGCGCATACGCCACCGCATAATGACCAAGCGTAC
GVGYG_3G3P_FP	CTTGGTCATTATCCTGTGCCTTATCCTCCTTACGTTCAGTTACCG
GVGYG_3G3P_RP	CTGAACGTAAGGAGGATAAGGCACAGGATAATGACCAAGCGTAC
mlaA_P151A FP	TACGTTCAGTTAGCGTTCTACGGTAGCTTCACGCTG
mlaA_P151A RP	GCTACCGTAGAACGCTAACTGAACGTAAGGCCC
Y^{147}VQL_to_4A FP	GGTTATGGGCCTGCGGCGGCGGCGCCGTTCTACGGTAGCTTCAC
Y^{147}VQL_to_4A RP	CTACCGTAGAACGGCGCCGCCGCCGCAGGCCCATAACCCACGCC
mlaA_Y40C FP	CAACCGCACCATGTGCAACTTCAACTTCAATG
mlaA_Y40C RP	AGTTGAAGTTGCACATGGTGCGGTTGAACCC
mlaA_D48C FP	CTTCAATGTATTATGCCCGTATATTGTTCGACC
mlaA_D48C RP	ACAATATACGGGCATAATACATTGAAGTTGAAG
mlaA_D92C FP	TAACTACTTCTTGCAGGGC TGC CCTTATCAGGGG
mlaA_D92C RP	GACCATCCCCTGATAAGG GCA GCCCTGCAAGAAG
mlaA_F114C FP	GGGATGGGCGGT TGCATTGATGTTGCAGGGATG
mlaA_F114C RP	GCAACATCAAT GCA ACCGCCCATCCCCAAAATGG
mlaA_F74C FP	GTTTGAGCAAC TGC ACTGGCAACCTTGAAGAACC
mlaA_F74C RP	CAAGGTTGCCAGT GCA GTTGCTCAAACCGTTACG
mlaA_G227C FP	TTCATCGCTAATTGCGGCGAACTCAAACCGCAG
mlaA_G227C RP	GTTTGAGTTCGCCGCAATTAGCGATGAAATCATG
mlaA_M84C FP	GAACCTGCGGTG TGC GTTAACTACTTCTTGCAGG
mlaA_M84C RP	GAAGTAGTTAAC GCA CACCGCAGGTTCTTCAAGG
mlaA_P209C FP	CAGTCGTCCGATTGCTATATTATGGTGCGCGAAG
mlaA_P209C RP	GCACCATAATATAGCAATCGGACGACTGACGCAG
mlaA_R193C FP	GGGATCGAAACCTGCGCTCAGCTGCTGGATTCC
mlaA_R193C RP	CAGCAGCTGAGCGCAGGTTTCGATCCCTTCAAGC
mlaA_T157C FP	CTACGGTAGCTTCTGCCTGCGTGATGACGGTGG
mlaA_T157C RP	TCATCACGCAG GCAGAAGCTACCGTAGAACGG
pCDFDuet-1_pelB_mlaA_ChisNdeI_Fwd	CGCT CAT ATG AAA TAC CTG CTG CCG ACC GCT GCT GC

pCDFDuet-1_FL_mlaA_ChisNdeI_Fwd	CGCT CAT ATG AAG CTT CGC CTG TCG
pCDFDuet-1_mlaA_AvrII Rev	AGAT CCT AGG TCA GTG GTG GTG GTG GTG GTG CTC GAG
pDSW206_ompC_NcoI Fwd	CGAT CC ATG GCA AAA GTT AAA GTA CTG TCC CTC C
pDSW206_ompC_HindIII Rev	CGCT AAG CTT TTA GAA CTG GTA AAC CAG ACC CAG AGC